Design of Wideband Compact Electric-Inductive-Capacitive (ELC) Inclusions for Metamaterials

Quang M. Nguyen, Theodore K. Anthony, and Amir I. Zaghloul

Abstract − Alternative designs for wideband compact electric-inductive-capacitive (ELC) inclusions, which can be used to construct metamaterials with desired high permittivity over a wide frequency band, are proposed and analyzed in this letter. To design a compact ELC inclusion, we incorporate a meander line (ML) into the conventional ELC structure. This helps to increase the equivalent inductance, which could lower the resonant frequency of the structure effectively. To expand the operating bandwidth, we introduce incremental variations in the dimensions of the ML. This helps create multiresonant responses of metamaterials, which could achieve high permittivity over a wide frequency band. The proposed design, which has an electrical size of about 1/14 of the wavelength in free space, can achieve approximately 40% more bandwidth than the single-resonance case for permittivity values greater than 3.5, or a 350 MHz bandwidth at 5 GHz. Experimental verifications were carried out to verify the design concept.

1. Introduction

Electromagnetic metamaterials, which were theorized by Veselago in 1968 [1], have gained significant research interest due to their novel electromagnetic properties not readily found in conventional materials. Metamaterials can be defined as periodic/nonperiodic arrays of subwavelength metallic or dielectric resonant inclusions. Examples of such resonant inclusions include thin wires [2], split-ring resonators (SRRs) [3], capacitively loaded loops [4], electric-inductive-capacitive (ELC) resonators [5], fishnets [6], and dielectric spheres, cylinders, or cubes [7]. Their electromagnetic responses can be accurately characterized by continuous bulk constitutive parameters, i.e., effective permittivity ε_r and permeability μ_r, which can be controlled via the shape, size, and material characteristics of the inclusions.

Metamaterials can be classified as epsilon-negative, mu-negative, or double negative (DNG) by superposition principles. Initial DNG structures, which were originally pioneered by Pendry et al., were based on SRRs and thin-wire media [2, 3]. However, thin-wire-media metamaterials have some serious drawbacks. They require continuous electrical connections between unit cells. When the long wire is cut at the

terminal of the unit cell to make each cell resonant individually, the resonance frequency is shifted to a much higher frequency. Additionally, it requires cross-cell electrical connections for 3D implementation, which may be problematic in the fabrication.

The ELC resonator, introduced by Schurig et al. [5], serves as an alternative route to customize the value of the permittivity. As a result, it can be used in conjunction with SRRs to construct DNG structures [8, 9]. ELC resonators have also been used in a wide range of applications, including absorbers [10], phase modulators [11], and polarizers [12]. Many compact ELC configurations have been introduced in recent years. These designs are based on the concept of raising the overall inductance and capacitance by changing the size of the inclusion, i.e., shortening gaps, lengthening wires, or redesigning the resonator pattern to accommodate a higher capacitance or inductance. Examples of such designs are listed as I-shaped, Z-shaped, meander-line, or thin square spiral resonators [13–17]. It should be noted that most of these redesigned structures do not exhibit pure electric resonance. In other words, they also provide magnetic and magnetoelectric inductions, especially when the incident magnetic field is perpendicular to the structure.

In this letter, we present a new compact ELC design used to construct metamaterials that achieve high permittivity over a wide frequency band. This can be done by incorporating a meander line into the conventional ELC structure. Unlike existing designs, the proposed design exhibits strong electric response with minimal magnetic and magnetoelectric effects. Furthermore, by introducing incremental variations in the dimensions of the meander line, we can broaden the operating bandwidth using the concept of multiresonant structures [18]. The design is simulated using the commercial electromagnetic simulator FEKO to obtain the scattering parameters S. Then the effective constitutive parameters, i.e., permittivity, permeability, and refractive index, are calculated through the retrieval process, which uses the S-parameters as the input [19–21].

2. Compact ELC Resonator Configurations

In this section, we discuss the design concept of the proposed compact ELC resonator configuration. In contrast to magnetic SRRs, an ELC resonator, as shown in Figure 1a, couples strongly to a uniform electric field and negligibly to a uniform magnetic field. Figure 1b shows the induced surface current distribution on the ELC, which indicates that the outer loops carry currents in opposite directions, resulting in no net magnetic moment. In the quasistatic limit, an ELC resonator can
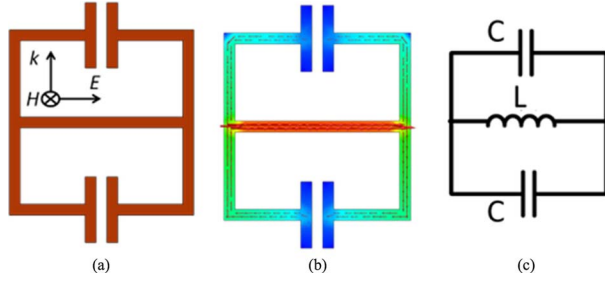
Figure 1. ELC resonator. (a) A variant that has two gaps on the exterior of the ELC, (b) the induced surface current on the ELC, and (c) an equivalent LC resonant circuit.

be presented in the form of an LC resonant circuit, as depicted in Figure 1c. As a rule of thumb, the resonance frequency of an ELC resonator can be tuned down by raising the overall inductance and capacitance. Typically, an ELC resonator and its variations (dual-gap design) have an electric size from one-sixth to one-eighth of the wavelength in vacuum.

A meander line (ML), as depicted in Figure 2a, is also a compact electric resonator due to the oscillation of currents induced in the perpendicular wires parallel to the incident electric field. For the continuous wires, the resonant frequency is zero, and for the cut wires it shifts to higher frequency due to the interruption in the wires causing the depolarized field. In the ML case, the resonant frequency is reduced proportionally to the number of arms. In other words, folding the wire in one unit cell will increase the overall inductance, resulting in the shift in frequency. As a result, the electric size of the meander line can be as short as one-tenth of the wavelength in vacuum [15]. Figure 2b also indicates that the energy is mainly focused in the middle of the ML.

A practical redesign of the compact ELC involves replacing the straight line in the center of a dual-gap ELC resonator with an ML, as illustrated in Figure 3. Theoretically, this helps to reduce the resonance frequency further by adding more inductance into the structure. To verify the design concept, we use the simulator FEKO. To simplify the problem, the substrate carrying the ML-loaded ELC resonator is assumed to be free space. The electromagnetic wave propagates along
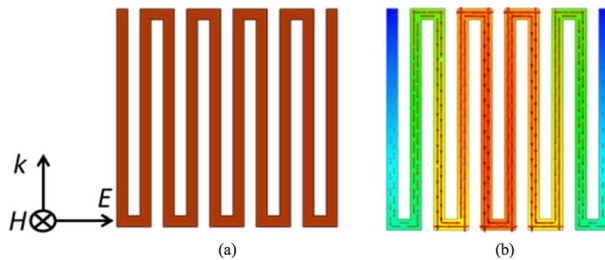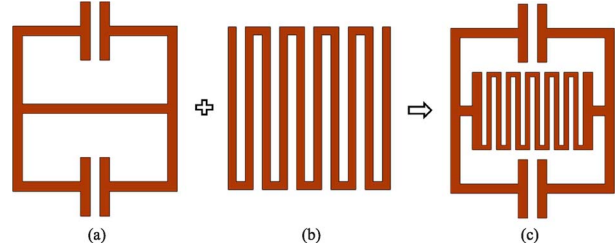

Figure 3. (a) A dual-gap ELC, (b) an ML, and (c) an ML-loaded ELC resonator.

the z-axis with an x-polarized electric field. Figure 4 shows the comparison of the S-parameters between an ML-loaded ELC and an ELC resonator. In this comparison, the model dimensions are chosen as $a = 6$ mm, $d = 4.25$ mm, $l_0 = 1.5$ mm, $l_1 = 2$ mm, and $w = g = 0.25$ mm. As can be seen, the ML-loaded ELC configuration exhibits a resonance frequency that is much lower than the one for the dual-gap ELC configuration. This frequency range becomes narrower and sharper as well, because of the stronger resonant intensity coming from the ML. The proposed design can achieve an electric size of about 1/14 of the wavelength in vacuum.

To quantify the electric response of the ML-loaded ELC resonator, we need to analyze its effective constitutive parameters. In this work, we consider its inclusion as dipole approximation, which leads to calculating polarizabilities, as described in [19, 20]. These polarizabilities are then substituted into the modified Clausius–Mossotti equations to find the bulk effective permittivity ε_r and permeability μ_r [21, 22].

3. Increasing Bandwidth of ML-Loaded ELC Resonators

The issue of narrow bandwidth in using metamaterial inclusions comes from the resonant nature built into the metamaterial concept. Several dual- or triple-band designs have been introduced and analyzed to address this issue. This can be done by embedding different sizes or shapes of the inclusion in one macrocell to create a structure that operates at different narrow frequency bands. In these designs, the operating bands are separated and the mutual coupling among the inclusions in one cell affects the overall performance of the structure.

In this section, we tackle the narrowband issue by using the concept of multiresonance as proposed in our previous work [18]. We present a macrocell design consisting of multi-unit cells with small incremental variations in dimension. Due to the nature of the ML-loaded ELC resonator, we only need to change the length of the ML to achieve this design concept. By keeping the same shape and overall size of the inclusion in each unit cell, we reduce unwanted coupling among them, which retains the desired performance of the
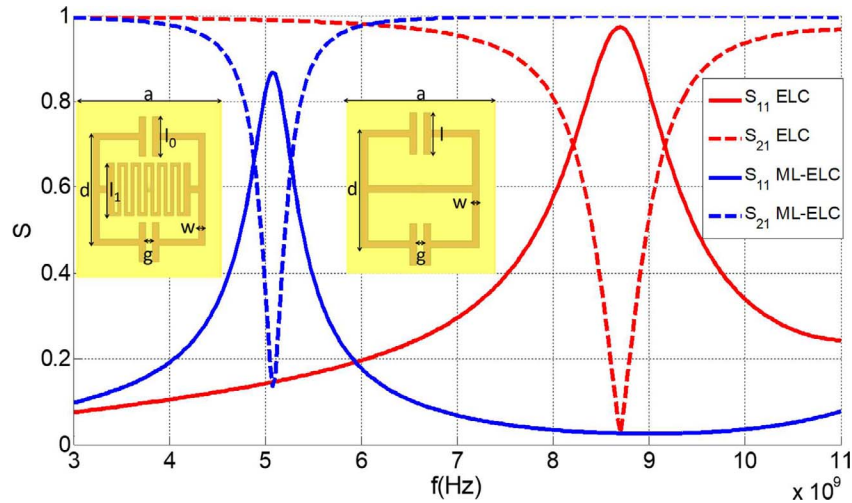

Figure 2. (a) The ML resonator and (b) the induced surface current on it.

Figure 4.   The comparison of S-parameters between an ML-loaded ELC resonator and an ELC resonator.

structure. To test this concept, we designed ML-loaded ELC macrocells consisting of five-unit cells, as shown in Figure 5. We varied the length of the ML across the five-unit cells in the macrocell with a step of 0.05 mm. The other dimensions were kept the same as described in the previous section.

S-parameters for the single-unit and multiunit cells were computed using FEKO, as illustrated in Figure 6a. As expected, the multi-unit cell design shows five mini peaks close to each other, around 5 GHz, in S_{11}, compared to a single peak for the single-unit cell design. This is a result of the small increments in the lengths of the ML across the five-unit cells. It should be noted that if there is no variation in the length of the ML across the unit cells in the macrocell, the S-parameters will be the same as for the single-unit cell. Using S-parameters as the input, the effective permittivity ε_r is calculated using the retrieval process, as shown in Figure 6b. For the single-unit cell design, we can only

achieve an approximately 250 MHz bandwidth at 5 GHz for $\varepsilon_r > 3.5$, due to the high resonant intensity coming from the ML. By introducing the multiresonance structure in the five-unit cell design, we can achieve an approximately 350 MHz bandwidth for $\varepsilon_r > 3.5$. This is 40% more bandwidth than with the single-unit cell.

4. Experimental Verification

Due to the constraints of waveguide-based measurement systems and the in-house fabrication facility, we had to scale up the dimensions of the proposed ML-loaded ELC design six times. The prototype dimensions became $a = 36$ mm, $d = 25.5$ mm, $l_0 = 9$ mm, $l_1 = 12$ mm, and $w = g = 1.5$ mm. We used RT/duroid 5880 (thickness = 3.175 mm) as the support base, with the ML-loaded ELC resonator printed on it. The measurement system was composed of a WR975 rectangular waveguide and an Agilent N5242A network analyzer. The fabricated samples had 7 strips, each 3.175 mm × 36 mm × 123.825 mm. They were placed in a sample holder, as depicted in Figure 7. The simulated and measured S-parameters of the single-unit-cell ML-loaded ELC are plotted in Figure 8. It should be noted that in the simulated model we built an actual WR975 waveguide, including a sample in the center, to closely match the measurement system. As we can see, the peak and dip in the S-parameters (around 750 MHz) indicate the resonant structure. There is a strong correspondence between measured and simulated data, except for a slight shift in the resonance frequency. The simulated results also do not capture the correct loss from the measured data. This results in a higher peak and lower dip (amplitude) in the S-parameters.

As expected, the retrieved permittivity using simulated and measured S-parameters have similar peaks around 750 MHz, as shown in Figure 9. The
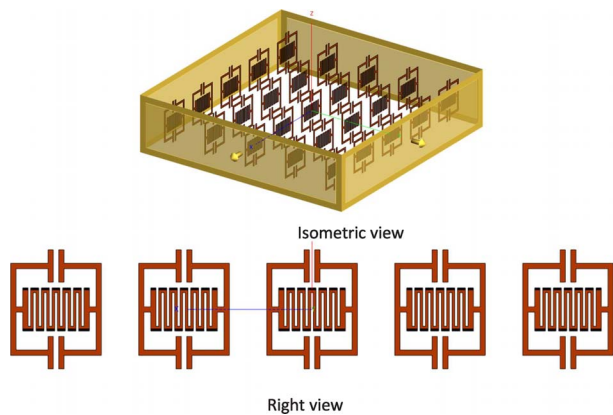

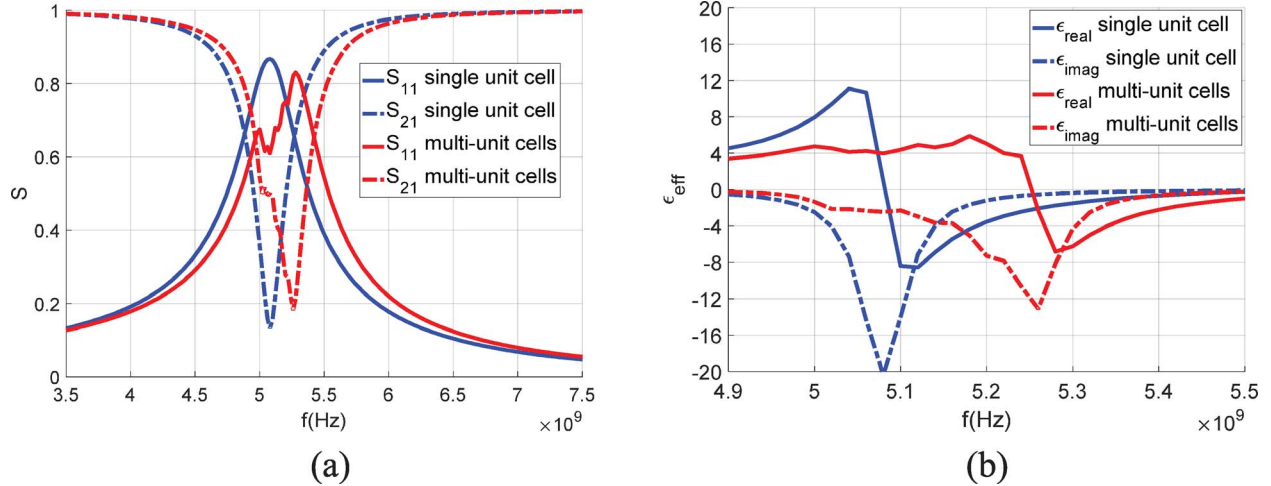Figure 5.   Macrocell of the ML-loaded ELC resonator consisting of five-unit cells.

Figure 6.   (a) The magnitudes of *S*-parameters of a macrocell versus a single-unit-cell ML-loaded ELC resonator. (b) The effective permittivity ε_r for a macrocell versus a single-unit-cell ML-loaded ELC resonator.

retrieved result is also consistent with the result from the proposed design (Figure 7), except that the resonance is at a much lower frequency due to the scaled-up version.

5. Conclusion

In this work, we presented a new ML-loaded ELC resonator, which can be used to construct metamaterials with desired high permittivity over a wide frequency band. By replacing the straight line in the center of a dual-gap ELC resonator with an ML, the proposed design can achieve an electric size of about 1/14 of the wavelength in vacuum. To widen the bandwidth, we used the concept of multiresonance. By incrementally varying the length of the ML across unit cells in a macrocell, we created multiresonance peaks; these peaks were very close to each other and yielded a continuously wide band in which the effective permittivity had a relatively high value. We achieved up to 40% more bandwidth than the single-resonance case. The scaled-up prototype was fabricated and measured. The measured data matched the simulated data.
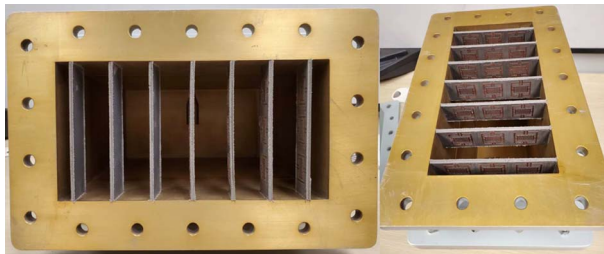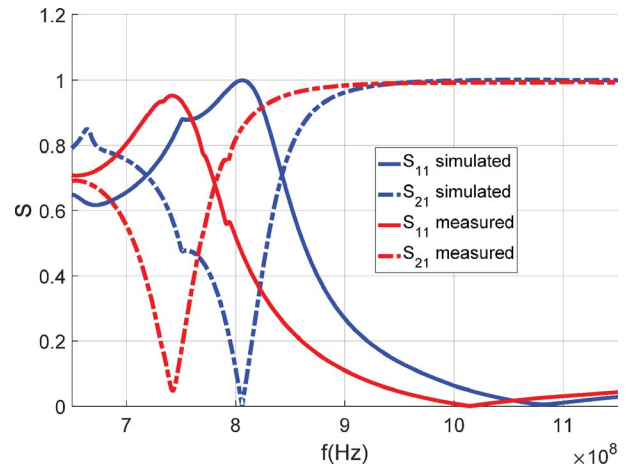

Figure 8.   Comparison of simulated and measured *S*-parameters (magnitude) for a single-unit-cell-loaded ELC resonator embedded in the host RT/duroid 5880.
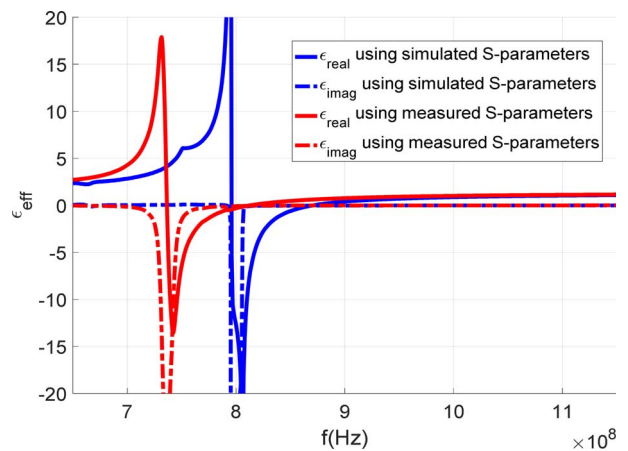

Figure 9.   The effective permittivity ε_r for the single-unit-cell ML-loaded ELC resonator using simulated *S*-parameters versus measured *S*-parameters.

Figure 7.   Fabricated ML-loaded ELC strip placed in sample holder.

6. References

1. V. G. Veselago, "The Electrodynamics of Substances With Simultaneously Negative Values of ϵ and μ, " *Soviet Physics Uspekhi*, **10**, 4, January-February 1968, pp. 509–514.

2. J. B. Pendry, A. J. Holden, W. J. Stewart, and I. Youngs, "Extremely Low Frequency Plasmons in Metallic Meso-structures," *Physical Review Letters*, **76**, 25, June 1996, pp. 4773–4776.

3. J. B. Pendry, A. J. Holden, D. J. Robbins, and W. J. Stewart, "Magnetism From Conductors and Enhanced Nonlinear Phenomena," *IEEE Transactions on Microwave Theory and Techniques*, **47**, 11, November 1999, pp. 2075–2084.

4. A. I. Zaghloul and Y. Lee, "Simulation of Refraction Focusing Using Negative-Refractive-Index Metamaterials," *2008 IEEE Antennas and Propagation Society International Symposium*, San Diego, CA, July 2008, pp. 1–4.

5. D. Schurig, J. J. Mock, and D. R. Smith, "Electric-Field-Coupled Resonators for Negative Permittivity Metamaterials," *Applied Physics Letters*, **88**, 4, January 2006, p. 041109.

6. M. Kafesaki, I. Tsiapa, N. Katsarakis, T. Koschny, C. M. Soukoulis, et al., "Left-Handed Metamaterials: The Fishnet Structure and Its Variations," *Physical Review B*, **75**, 23, June 2007, p. 235114.

7. P. Moitra, B. A. Slovick, Z. G. Yu, S. Krishnamurthy, and J. Valentine, "Experimental Demonstration of a Broadband All-Dielectric Metamaterial Perfect Reflector," *Applied Physics Letters*, **104**, 17, April 2014, p. 171102.

8. R. Liu, A. Degrion, J. J. Mock, and D. R. Smith, "Negative Index Material Composed of Electric and Magnetic Resonators," *Applied Physics Letters*, **90**, 26, June 2007, p. 263504.

9. T. D. Karamanos, A. I. Dimitriadis, and N. V. Kantartzis, "Compact Double-Negative Metamaterials Based on Electric and Magnetic Resonators," *IEEE Antennas and Wireless Propagation Letters*, **11**, May 2012, pp. 480–483.

10. N. I. Landy, S. Sajuyigbe, J. J. Mock, D. R. Smith, and W. J. Padilla, "Perfect Metamaterial Absorber," *Physical Review Letters*, **100**, 20, May 2008, p. 207402.

11. H.-T. Chen, W. J. Padilla, M. J. Cich, A. K. Azad, R. D. Averitt, et al., "A Metamaterial Solid-State Terahertz Phase Modulator," *Nature Photonics*, **3**, 3, 2009, pp. 148–151.

12. J. Y. Chin, M. Lu, and T. J. Cui, "Metamaterial Polarizers by Electric-Field Coupled Resonators," *Applied Physics Letters*, **93**, 25, December 2008, p. 251903.

13. W. Withayachumnankul, C. Fumeaux, and D. Abbott, "Compact Electric-LC Resonators for Metamaterials," *Optics Express*, **18**, 25, December 2010, pp. 25912–25921.

14. S. Bhattacharyya and K. V. Srivastava, "Ultra Thin Metamaterial Absorbers Using Electric Field Driven LC (ELC) Resonator Structure," PIERS Proceedings, Kuala Lumpur, Malaysia, March 2012, pp. 314–317.

15. W. X. Tang, H. Zhao, X. Zhou, J. Y. Chin, and T.-J. Cui, "Negative Index Material Composed of Meander Line and SRRs," *Progress in Electromagnetics Research B*, **8**, 2008, pp. 103–114.

16. P. W. Kolb, T. S. Salter, J. A. McGee, H. D. Drew, and W. J. Padilla, "Extreme Subwavelength Electric GHz Metamaterials," *Journal of Applied Physics*, **110**, 5, September 2011, p. 054906.

17. A. Dhouibi, S. N. Burokur, A. de Lustrac, and A. Priou, "Z-Shaped Meta-Atom for Negative Permittivity Metamaterials," *Applied Physics A: Materials Science & Processing*, **106**, 1, 2012, pp. 47–51.

18. Q. M. Nguyen, A. I. Zaghloul, T. K. Anthony, and S. J. Weiss, "Using Multiple Resonances to Widen the Band for High-Permeability Spiral-Pair Metamaterials," *IEEE Antennas and Wireless Propagation Letters*, **18**, 5, March 2019, pp. 1026–1030.

19. A. D. Scher and E. F. Kuester, "Extracting the Bulk Effective Parameters of a Metamaterial via the Scattering From a Single Planar Array of Particles," *Metamaterials*, **3**, 1, March 2009, pp. 44–55.

20. T. D. Karamanos, A. I. Dimitriadis, and N. V. Kantartzis, "Robust Technique for the Polarisability Matrix Retrieval of Bianisotropic Scatterers via Their Reflection and Transmission Coefficients," *IET Microwaves, Antennas & Propagation*, **8**, 15, December 2014, pp. 1398–1407.

21. T. D. Karamanos, S. D. Assimonis, A. I. Dimitriadis, and N. V. Kantartzis, "Effective Parameter Extraction of 3D Metamaterial Arrays via First-Principles Homogenization Theory," *Photonics and Nanostructures—Fundamentals and Applications*, **12**, 4, August 2014, pp. 291–297.

22. A. Alù, "First-Principles Homogenization Theory for Periodic Metamaterials," *Physical Review B*, **84**, 7, August 2011, p. 075153.